

Supplementary Information

Nonzero Berry curvature dipole, magnetic gapped edge states and persistent spin texture in a rotational symmetry preserved van der Waals magnetic topological insulator

Saransha Mohanty¹, Anil Kumar Singh¹, Liyenda Gogoi¹ and Pritam Deb^{1*}

*Corresponding authors

¹ Advanced Functional Materials Laboratory, Department of Physics, Tezpur University (Central University), Tezpur 784028, India

*Email: pdeb@tezu.ernet.in

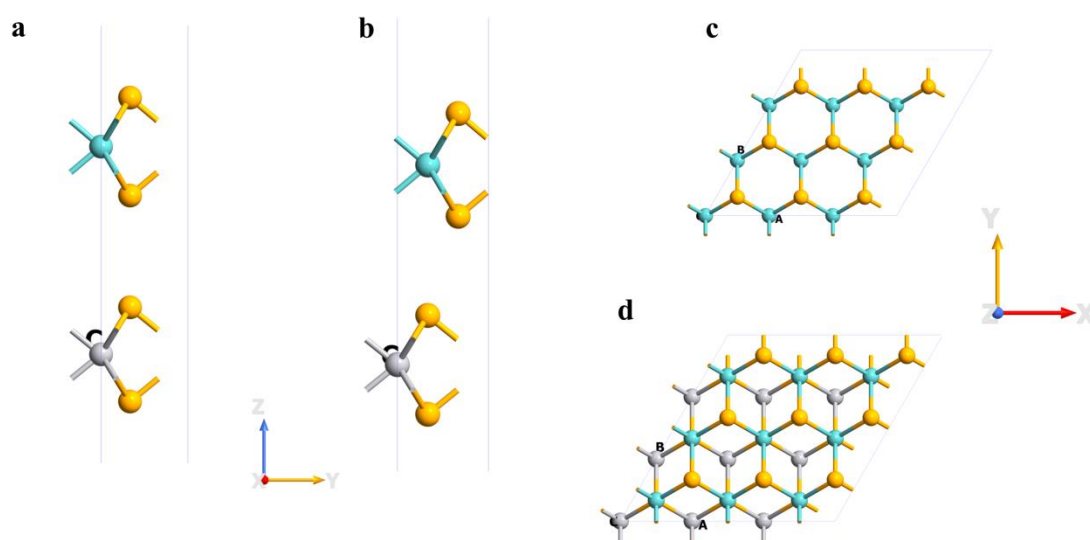


Figure S1: Side profile of (a) AA, (b) AB stacked vdW unit cell of 1H-MoSe₂/1H-VSe₂ system, top view of (c) AA and (d) AB stacked 4 × 4 × 1 supercell 1H-MoSe₂/1H-VSe₂ vdW heterostructure. Green, Silver and Yellow balls correspond to Molybdenum (Mo), Vanadium (V) and Selenium (Se) atoms.

In AA stacked geometric configuration, MoSe₂ atoms directly lay atop of VSe₂ atoms and appears as a single layer when viewed from top Fig.S1(c). In AB-stacked atomic configurations, the Mo-atom lay on top of Se atom belonging to VSe₂ monolayer. The top view of AB stacked cell (Fig.S1(d)) displays the appearance of two distinct monolayer sheets. The lattice constants of MoSe₂ and VSe₂ monolayers are 3.33Å and 3.37Å respectively with lattice mismatch of 1.1% in vdW heterostructure.

The formation energy ($E_{formation}$) of the AA and AB stacked unit cells is calculated following the equations $E_{formation} = (E_{heterostructure} - E_{VSe_2} - E_{MoSe_2})/n$,

where $E_{heterostructure}$, E_{MoSe_2} and E_{VSe_2} represent energy of heterobilayer unit cell, MoSe₂ and VSe₂ monolayer systems respectively and n as the total number of atoms in the heterostructure unit cell

For AA stacked geometric configurations, the obtained energy values are $E_{heterostructure} = -456.48804167 \text{ Ry}$, $E_{VSe_2} = -232.30819032 \text{ Ry}$ and $E_{MoSe_2} = -224.16981345 \text{ Ry}$.

Similarly, for AB stacked heterobilayer, the energy values corresponding to respective systems are $E_{heterostructure} = -456.50230970 \text{ Ry}$, $E_{VSe_2} = -232.31308861 \text{ Ry}$ and $E_{MoSe_2} = -224.17663714 \text{ Ry}$.

The calculated binding energy values are $E_{formation}^{AA} = -22.75 \text{ meV}$, and $E_{formation}^{AB} = -28.52 \text{ meV}$ respectively. We observe AB stacked heterobilayer is more stable in comparison to its AA stacked counterpart unit cell due to its lower formation energy.

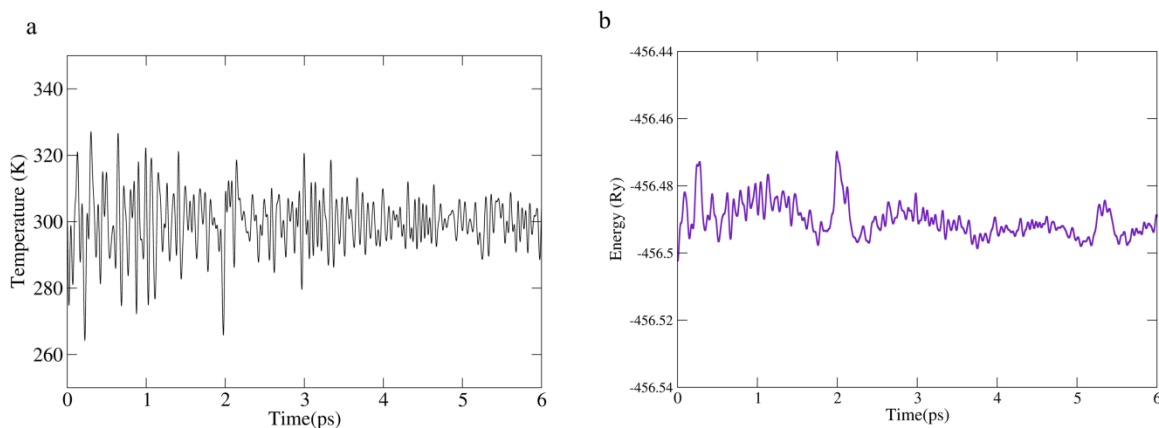


Figure S2: AIMD simulations of 1H-MoSe₂/1H-VSe₂ vdW heterostructure. Variation of (a) temperature and (b) energy with respect to time. The time is measured in picosecond (ps).

The Fig.S2(a-b) shows both thermal and energy dependent dynamic stability of the developed vdW heterostructure. We observe that with time, the temperature saturates near to room temperature (300K) (see Fig.S2(a)) whereas there exist negligible variation in energy values (Fig.S2(b)) with increase in time. The above observations portray the room temperature stability of the developed systems.

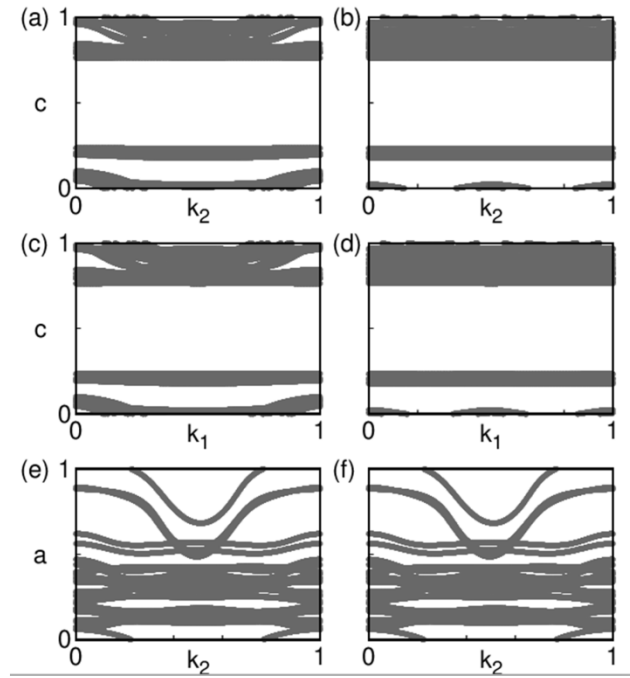


Figure S3: The calculated Chern number in the six planes of in Brillouin zone in full closed momentum surface (i.e., 0 to 1). The Chern numbers are (a) $k_1 = 0.0$, k_2 - k_3 plane: $C = 0$. (b) $k_1 = 0.5$, k_2 - k_3 plane: $C = 0$. (c) $k_2 = 0.0$, k_1 - k_3 plane: $C = 0$. (d) $k_2 = 0.5$, k_1 - k_3 plane: $C = 0$. (e) $k_3 = 0.0$, k_1 - k_2 plane: $C = 1$. (f) $k_3 = 0.5$, k_1 - k_2 plane: $C = 1$

In Fig.S3(e-f), we observe that the Chern number for $k_3 = 0$ and $k_3 = 0.5$ is $C = 1$, which further supports emergence of topological characteristics of the system.

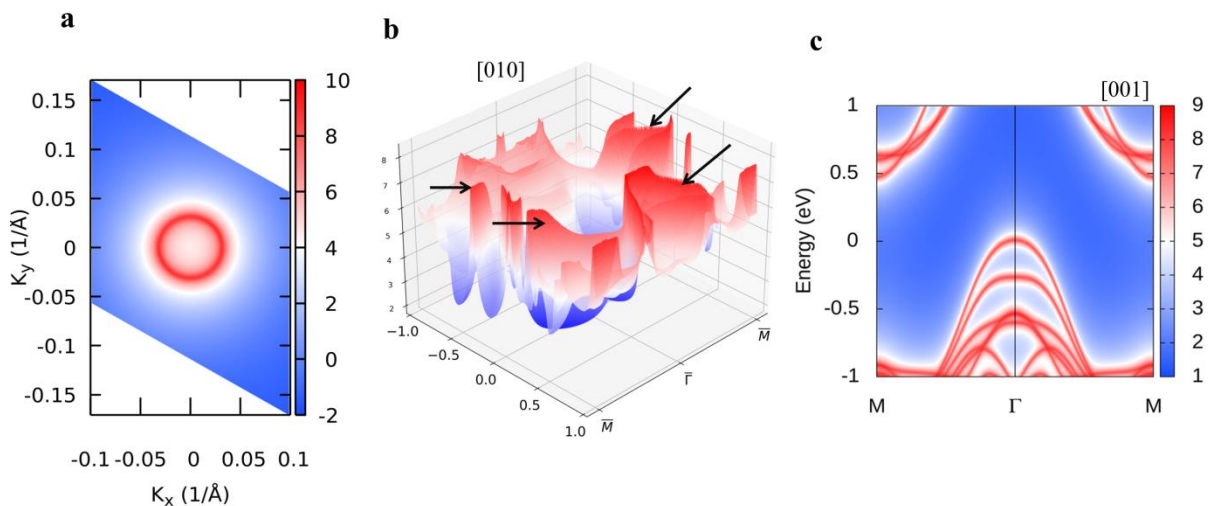


Figure S4: (a) Fermi arc along $[001]$ direction, (b) 3D view of emerged edge states along $[010]$ direction and (c) edge states along $[001]$ direction. The black arrows indicate the emerged edge states.

In [001] direction, the emerged edge states are projected onto the bulk band spectrum of the system.

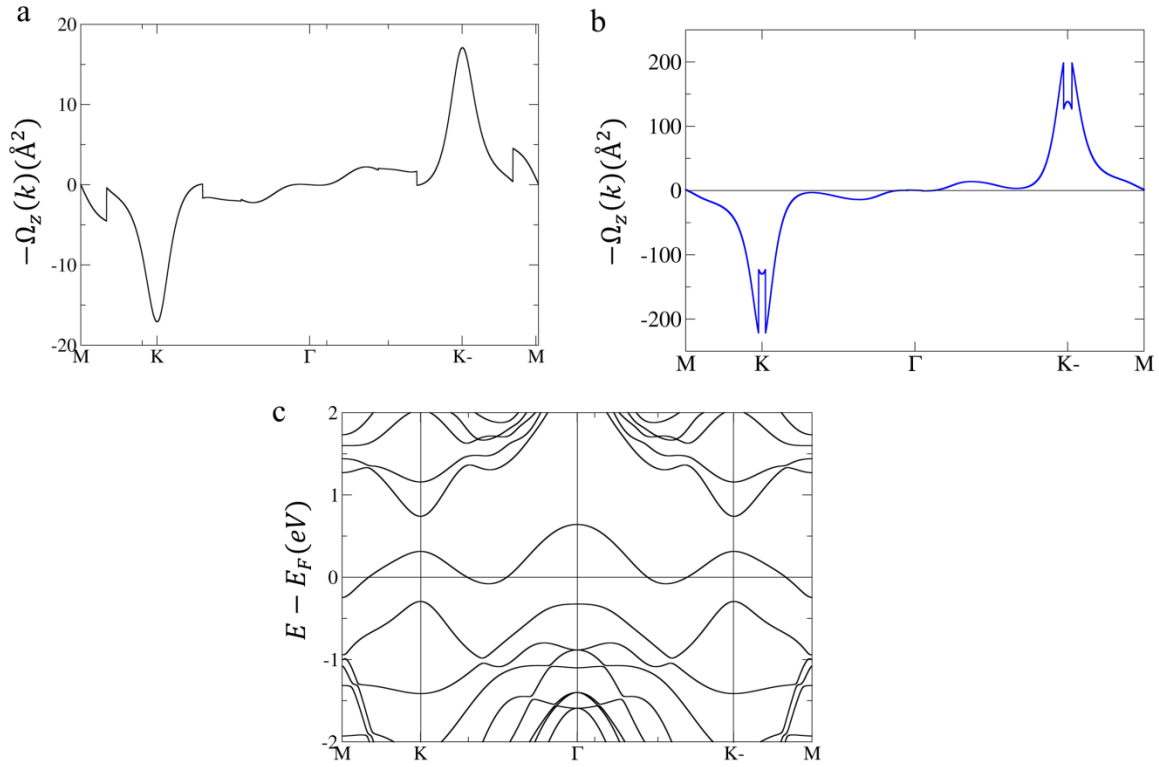


Figure S5: Berry curvature for (a) nonmagnetic, (b) ferromagnetic vdW 1H-MoSe₂/1H-VSe₂ system direction respectively, (c) energy band diagram for nonmagnetic 1H-MoSe₂/1H-VSe₂ vdW heterostructure.

For nonmagnetic vdW 1H-MoSe₂/1H-VSe₂ heterostructure, Fig.S5(a) shows equal magnitude of Berry curvature peak of strength 17.2 \AA^2 , whereas with introduction of magnetism as in Fig. S5(b), we have observed unequal distribution of Berry curvature in the system. Fig.S5(c), demonstrates the energy band diagram for nonmagnetic 1H-MoSe₂/1H-VSe₂ vdW system, suggesting its metallic character.

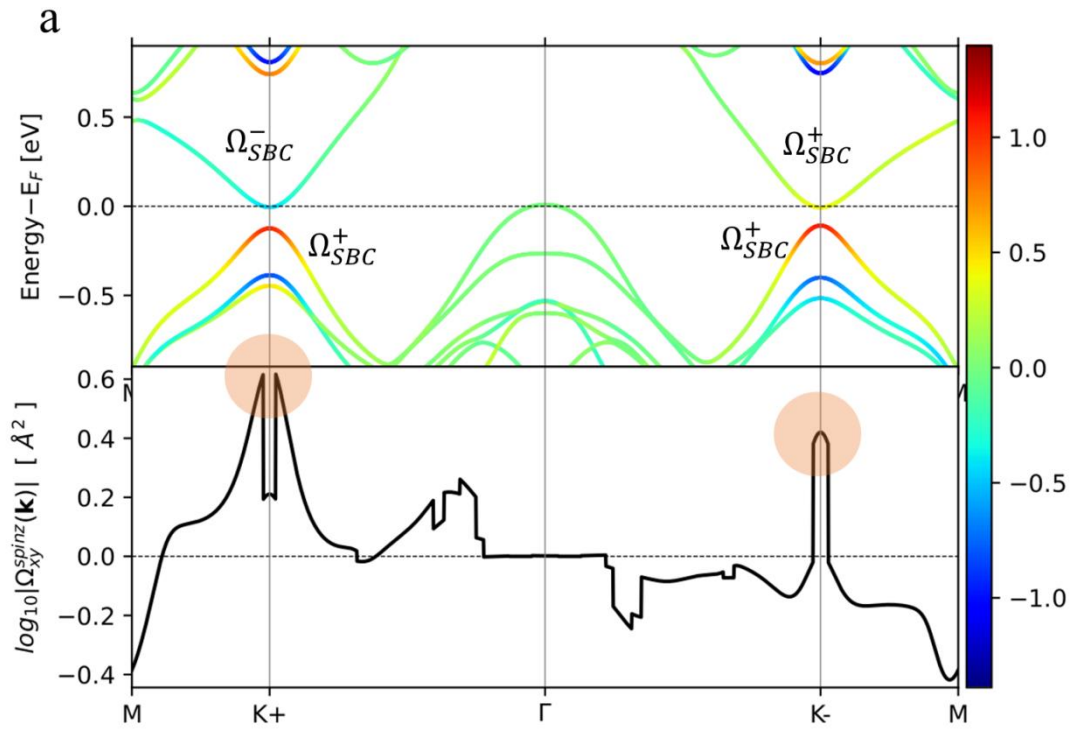


Figure S6: k-resolved spin Berry curvature (Ω_{SBC}) projected on (a) electronic band diagram and (b) in logarithmic scale. Ω_{SBC}^+ and Ω_{SBC}^- corresponds to spin Berry curvature of opposite spin states. The marked circle corresponds to emerged spin Berry curvature spikes at two K valleys.

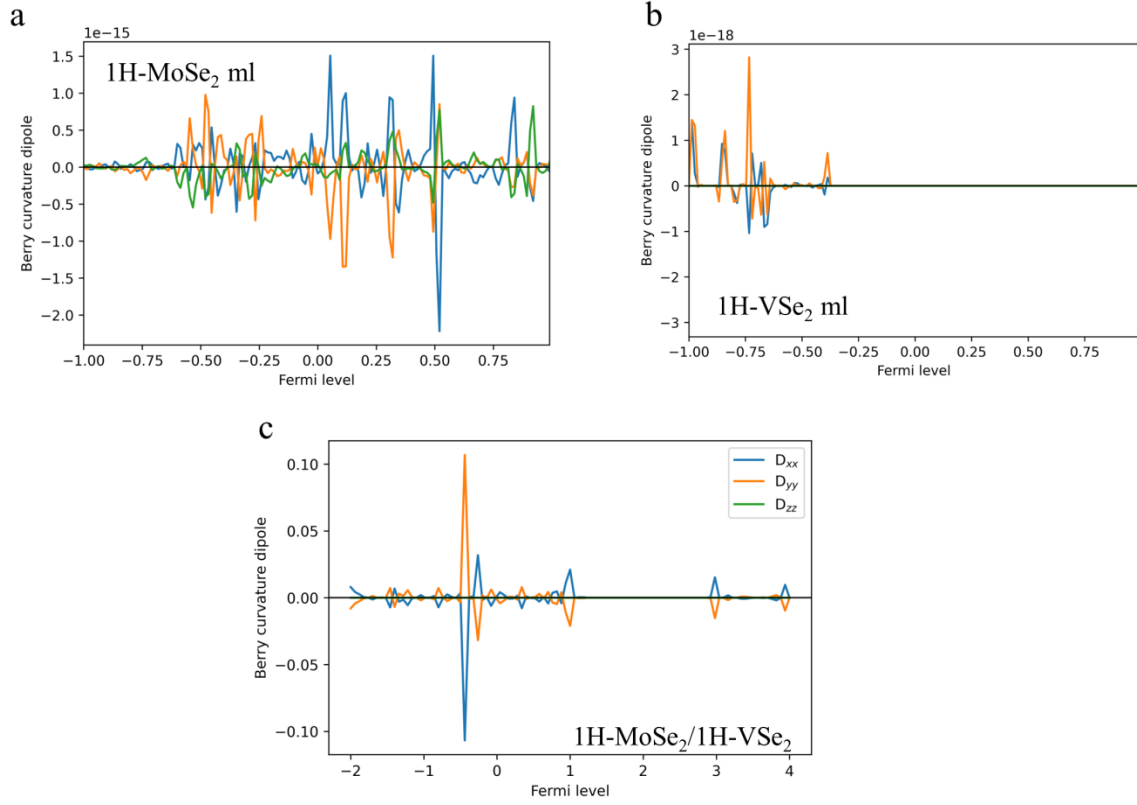


Figure S7: Berry curvature dipole for (a) monolayer 1H-MoSe₂, (b) 1H-VSe₂ monolayer and (c) 1H-MoSe₂/1H-VSe₂ vdW heterostructure.

We observe the strength of Berry curvature dipole components in Fig.S7 (a-b) for both monolayer 1H-MoSe₂ and 1H-VSe₂ is approximately of the order of 10^{-15} , which is equivalent to zero. However, for vdW heterostructure we observe appearance of non-zero Berry curvature dipole components.